Dalton Transactions

Accepted Manuscript

ROYAL SOCIETY OF CHEMISTRY

www.rsc.org/dalton

Journal Name

ARTICLE

Luminescent europium and terbium complexes of dipyridoquinoxaline and dipyridophenazine ligands as photosensitizing antenna: structures and biological perspectives†

Received 00th January 20xx,
Accepted 00th January 20xx

DOI: 10.1039/x0xx00000x

www.rsc.org/

Srikanth Dasari and Ashis K. Patra*

The europium(III) and terbium(III) complexes, namely [Eu(dpq)(DMF)$_2$(NO$_3$)$_3$] (**1**), [Eu(dppz)$_2$(NO$_3$)$_3$] (**2**), [Tb(dpq)(DMF)$_2$Cl$_3$] (**3**), and [Tb(dppz)(DMF)$_2$Cl$_3$] (**4**), where dipyrido[3,2-*d*:2′,3′-*f*]quinoxaline (dpq in **1** and **3**), dipyrido[3,2-*a*:2′,3′-*c*]phenazine (dppz in **2** and **4**) and *N*,*N*′-dimethylformamide (DMF) have been isolated, characterized from their physicochemical data, luminescence studies and their interaction with DNA, serum albumin protein and photo-induced DNA cleavage activity are studied. The X-ray crystal structures of complexes **1**-**4** showing discrete mononuclear Ln^{3+}-based structures. The Eu^{3+} in [Eu(dpq)(DMF)$_2$(NO$_3$)$_3$] (**1**) and [Eu(dppz)$_2$(NO$_3$)$_3$] (**2**) as [Eu(dppz)$_2$(NO$_3$)$_3$].dppz (**2a**), adopts a ten-coordinated bicapped dodecahedron structure with a bidentate *N*,*N*-donor dpq ligand, two DMF and three NO$_3^-$ anions in **1** and two bidentate *N*,*N*-donor dppz ligands and three NO$_3^-$ anions in **2**. Complexes **3** and **4** show a seven-coordinated mono-capped octahedron structure where Tb^{3+} containing a bidentate dpq/dppz ligands, two DMF and three Cl$^-$ anions. Complexes are highly luminescent in nature indicating efficient photo-excited energy transfer from dpq/dppz antenna to Ln^{3+} to generate long-lived emissive excited states for characteristic $f \rightarrow f$ transitions. The time-resolved luminescence spectra of the complexes **1**-**4** shows typical narrow emission bands attributed to $^5D_0 \rightarrow {}^7F_J$ and $^5D_4 \rightarrow {}^7F_J$ f-f transitions of Eu^{3+} and Tb^{3+} ions respectively. Number of inner-sphere water molecules (q) were determined from luminescence lifetime measurements in H$_2$O and D$_2$O confirming ligand-exchange reactions with water in solution. The complexes display significant binding propensity to the CT-DNA giving binding constant values in the range of 1.0 x 10^4 – 6.1 x 10^4 M^{-1} in the order **2, 4** (dppz) >**1, 3** (dpq). DNA binding data suggest DNA groove binding with partial intercalation nature of the complexes. All the complexes also show binding propensity ($K_{BSA} \sim 10^5$ M^{-1}) to bovine serum albumin (BSA) protein. The intensity of the time-gated luminescence spectral bands enhances significantly with increasing DNA concentration in aqueous buffer medium due to displacement of bound water upon interaction with DNA and thus reducing non-radiative quenching through O-H oscillator. Complexes **1–4** efficiently cleave supercoiled (SC) ds-DNA to its nicked circular (NC) form on exposure to UV-A light of 365 nm via formation of singlet oxygen ($^1O_2$) and hydroxyl radical (HO$^\bullet$) as reactive oxygen species at micromolar concentration under physiological condition.

Introduction

Development of metal complexes that bind and cleave DNA under physiological conditions are of great current interests towards developing models for restriction enzymes, foot-printing agents, diagnostic agents, and metal-based chemotherapeutic agents.[1-10]

Photodynamic therapy (PDT) of cancer has emerged as a powerful alternative for treating cancer due to its non-invasive and selective nature in which the photo-activatable prodrug becomes toxic to cancer cells only on photo-irradiation leaving the healthy cells unaffected.[11-13] Therapeutic efficacy of PDT is mediated by generation of cytotoxic reactive oxygen species (ROS) like singlet oxygen ($^1O_2$), hydroxyl (HO$^\bullet$) radical and/or superoxide ($O_2^{\bullet-}$) radicals on photoactivation of the photosensitizer via a type-II or type-I pathways.[14-17] Light-activated production of cytotoxic ROS causes oxidative cell death only to the region of irradiation. The PDT offers a high degree of spatiotemporal selectivity which can be fine-tuned by judicious choice of the photosensitizer, excitation wavelength and mode of application. Lanthanide compounds are of considerable interest as contrast agents in magnetic resonance imaging (MRI) and as luminescent bioprobes and bioresponsive cellular imaging agents.[18-24] Free lanthanide ions and their complexes are known as remarkably effective catalysts for the hydrolysis of phosphodiester bonds in nucleic acids due to their strong Lewis acidity, higher charge density and rapid ligand exchange rates for potential applications as artificial nucleases.[25-28] The acceleration of phoshodiester hydrolysis rate by Ce^{4+}, Tm^{3+}, Yb^{3+} and Lu^{3+} is almost 10^8-10^{12} fold. Lanthanide complexes having varied coordination geometries ranging from seven to ten coordinated are suitable for designing

Department of Chemistry, Indian Institute of Technology Kanpur, Kanpur 208016, Uttar Pradesh, India. E-mail: akpatra@iitk.ac.in

†Electronic Supplementary Information (ESI) available: Cyclic voltammograms; unit cell packing diagrams; crystallographic data tables; luminescence spectra; lifetime measurements; DNA and protein binding plots; DNA cleavage data. For ESI and crystallographic data in CIF or other electronic format see DOI: 10.1039/x0xx00000x.

multimodal DNA photo-cleavage agents for theranostic applications utilizing their efficient magnetic relaxation (MRI) or time-resolved luminescence properties.[18,29] The remarkable redox stability of lanthanides in trivalent oxidation state is also advantageous in presence of indigenous cellular thiols, ascorbates and reducing hypoxic conditions present in cancerous cells. While several 3d-5d transition metal-based photoacivated complexes are reported,[30-35] there are only few examples of photocytotoxic lanthanide complexes of texaphyrins and *N*,*N*-donor heterocyclic bases were reported for PDT applications.[36-39] Lutetium(III) texaphyrin (LUTRIN®) shows remarkable phototherapeutic effect for the treatment of breast cancer, atherosclerosis and age-related macular degeneration on activation at tissue-penetrating far-red light of 732 nm.[36] Chakravarty et al. have systematically studied photo-induced DNA cleavage and photocytotoxicity activity of a series of La^{3+} and Gd^{3+} complexes of planar phenanthroline, pyridylphenanthroline and substituted terpyridine bases as photosensitizer with UV-A light involving formation of singlet oxygen ($^1O_2$) and hydroxyl radical (•OH) as reactive oxygen species.[38,39] This work originate from our interest to design emissive europium and terbium complexes and study their interactions with DNA and serum proteins and photo-induced DNA cleavage activity.

Herein, we report the synthesis, characterization, crystal structures, photophysical studies, DNA and BSA binding, time-gated DNA sensing and photo-induced DNA cleavage activity of the luminescent Eu^{3+} and Tb^{3+} complexes, viz. $[Eu(dpq)(DMF)_2(NO_3)_3]$ (**1**), $[Eu(dppz)_2(NO_3)_3]$ (**2**), $[Tb(dpq)(DMF)_2Cl_3]$ (**3**), and $[Tb(dppz)(DMF)_2Cl_3]$ (**4**), where dpq = dipyrido[3,2-*d*:2′,3′-*f*]quinoxaline (in **1** and **3**), and dppz = dipyrido[3,2-*a*:2′,3′-*c*]phenazine (in **2** and **4**) and DMF = *N*,*N*′-dimethylformamide (Scheme 1). Complexes **1**, **2** as **2·dppz·Et$_2$O**, **3** and **4** were structurally characterized by X-ray crystallography. The choice of dpq and dppz ligands as photosensitizing antenna is based on their ability to generate photo-induced $^3(n\text{-}\pi^*)$ and/or $^3(\pi\text{-}\pi^*)$ states which in turn transfer its energy to molecular oxygen to form reactive oxygen species that causes oxidative damage to DNA. Upon photoexcitation, coordinated dpq and dppz antenna moieties show efficient energy transfer to Ln^{3+} ion for generating emissive excited states of Eu^{3+} and Tb^{3+}. There are earlier reports on application of analogous tetraazatriphenylene sensitizing chromophores as efficient photosensitizer for lanthanide emission.[40] We have observed efficient photo-induced DNA cleavage activity of complexes **1**-**4** under low energy UV-A light of 365 nm involving formation of singlet oxygen ($^1O_2$) in a type-II pathway and hydroxyl radicals (•OH) in a photo-redox pathway.

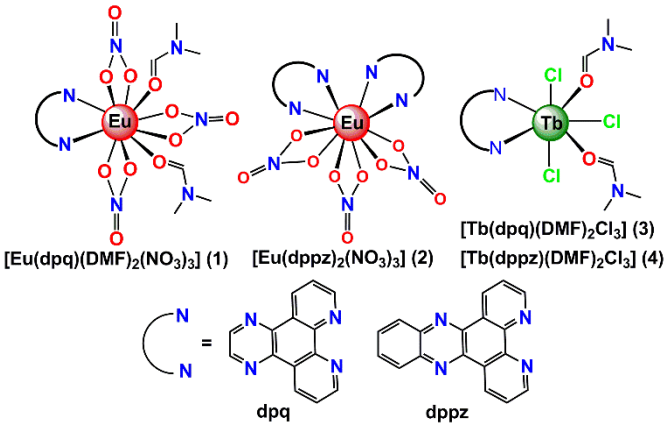

Scheme 1 Complexes **1**-**4** and *N*,*N*-donor heterocyclic bases used as photosensitizing antenna moiety.

Results and discussion

Synthesis and general aspects

Lanthanide(III) complexes namely $[Eu(dpq)(DMF)_2(NO_3)_3]$ (**1**), $[Eu(dppz)_2(DMF)_2(NO_3)_3]$ (**2**), $[Tb(dpq)(DMF)_2Cl_3]$ (**3**), and $[Tb(dppz)(DMF)_2Cl_3]$ (**4**) of dipyrido[3,2-*d*:2′,3′-*f*]quinoxaline (dpq in **1** and **3**), dipyrido[3,2-*a*:2′,3′-*c*]phenazine (dppz in **2** and **4**) (Scheme 1), are prepared using a general synthetic procedure by reacting a methanolic solution of $Eu(NO_3)_3{\cdot}5H_2O$ or $TbCl_3{\cdot}6H_2O$ with the corresponding phenanthroline base in boiling methanol. All the complexes have been isolated in good yields and characterized by elemental analysis, FT-IR, UV-visible spectra, ESI-MS spectral techniques and structural determination form single crystal X-ray crystallography. Selected physicochemical data are given in Table 1. The molar conductivity values of 82-122 Scm^2M^{-1} suggests 1:1 electrolytic nature of the complexes in aqueous DMF. The positive ion mode ESI-MS analysis of the complexes **1**-**4** showed respective molecular ion peaks in solution. The FT-IR spectral data indicate the presence of bidentate coordination of nitrate to the Eu^{3+} center from the appearance of a medium to strong intensity band at ~1400 cm^{-1}. The UV-visible spectra of the complexes in DMF show an intense ligand centered $\pi\rightarrow\pi^*$ transition at 272 nm (Fig. 1). The dpq complexes **1** and **3** exhibit a shoulder around 340 nm could be assigned to $n\rightarrow\pi^*$ transition involving the quinoxaline moiety.

Table 1 Selected physicochemical data and DNA/BSA binding parameters for the complexes **1**-**4**

Complex	IR[a]/cm^{-1}, $\nu(NO_3)$	λ_{max}[b]/ nm, (ε/$M^{-1}cm^{-1}$)	Λ_M[c]/S cm^2 M^{-1}	K_b[d] / M^{-1}	K_{app}[e]/ M^{-1}	K_{BSA}[f]/ M^{-1}
1	1470, 1405, 1287	273 (77360), 340 (18300)	102	1.0 (±0.2) × 10^4	4.83 × 10^6	2.12(±0.2) x 10^5
2	1497, 1419, 1309	376 (28970), 365 (29000) 272 (98180)	122	4.9 (±0.3) × 10^4	6.03 × 10^6	2.07 (±0.4) x 10^5
3	-	273 (75650), 340 (18800)	82	2.7 (±0.3) × 10^4	4.56 × 10^6	1.64 (±0.3) x 10^5
4	-	376 (27650), 365 (27680) 272 (93180)	89	6.1 (±0.3) × 10^4	5.00 × 10^6	1.35 (±0.1) x 10^5

[a]In KBr phase. [b]UV-visible spectra in DMF. [c]Molar conductance in aqueous DMF (1:9) at 298 K. [d]K_b, intrinsic equilibrium DNA binding constant. [e]K_{app}, apparent DNA binding constant. [f]K_{BSA} , Stern-Volmer quenching constant for BSA fluorescence.

Journal Name

ARTICLE

The dppz complexes **2** and **4** show two bands at 365 and 376 nm attributed to the $n\rightarrow\pi^*$ transitions of the phenazine moiety.[41] Absorption spectral traces for the complexes in DMF was recorded at 25 °C for 4 h do not show any significant spectral changes in DMF solution (Fig. S1, ESI†). The emission bands observed for the complexes correspond to the $^5D_0\rightarrow{}^7F_J$ (J = 0-4) and $^5D_4\rightarrow{}^7F_J$ (J = 6-3) *f-f* transitions for Eu^{3+} and Tb^{3+} respectively (Figs. S8-S11, ESI†). In aqueous media the complexes undergo ligand-exchange reactions via displacement of bound DMF, NO_3^- or Cl^- anions by water molecules. To understand the solution state structure of the complexes in aqueous media we have determined the number of inner-sphere water molecules (q) of the complexes using luminescence lifetimes in H_2O and D_2O via modified Horrock's equation[42] (see ESI†). The hydration values ($q\approx$ 4-6) obtained for complexes **1**-**4** were consistent with ligand displacement reaction by water. Increased excited state lifetime of the complexes in D_2O compared to in DMF or H_2O also suggests this ligand exchange phenomena in solution. Moreover, lower overall quantum yield of the complexes observed in water than in DMF also indicate coordination of water molecule to lanthanide ions. The nonradiative quenching via O-H oscillators of H_2O lowers the excited state lifetime and thus emission quantum yields in solution (Tables S6, S7, ESI†). The $[Tb(dppz)(DMF)_2Cl_3]$ (**4**) complex, due to presence of a low-lying triplet state of dppz is susceptible to quenching by O_2.[40b,c] We observed almost twice excited state lifetime in degassed aqueous solution (τ = 0.667 ms) than in aerated solution (τ = 0.353 ms). The europium complexes of dpq and dppz (**1** and **2**) are redox active showing a quasi-reversible $Eu^{3+/2+}$ couple at $E_{1/2}$ = –0.627 V (ΔE_p = 204 mV) for **1** (Fig. 1) and a cathodic peak (E_{pc}) at –0.714 V vs. Ag/AgCl with poor reversibility for **2** in DMF–0.1M TBAP. For terbium complexes the redox processes are primarily due to ligand centered implying stability of terbium in trivalent oxidation state. The dpq complexes (**1**, **3**) show ligand based irreversible redox couples near -1.30 V and -1.51 V. The dppz complexes **2** and **4** show a quasi-reversible voltammograms at $E_{1/2}$ = –1.10 V (ΔE_p = 85 mV) as observed in analogous lanthanide complexes (Figs. S2-S4, ESI†).[38b, 43]

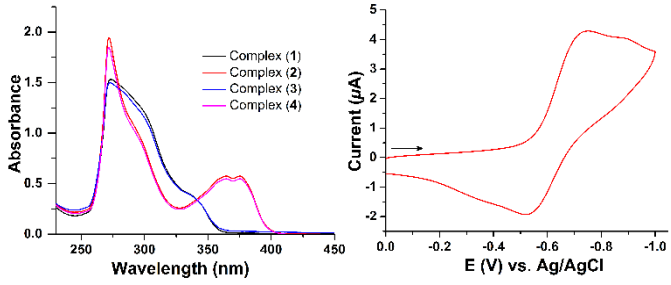

Fig. 1 UV-visible spectra of complexes **1**-**4** in DMF at 298 K (left). Cyclic voltammogram of complex **1** in DMF-0.1M TBAP with a scan speed of 50 mV s^{-1} (right).

X-ray crystal structures

All the complexes, *viz.* $[Eu(dpq)(DMF)_2(NO_3)_3]$ (**1**), $[Eu(dppz)_2(NO_3)_3]$ (**2**) as **2·dppz·Et₂O**, $[Tb(dpq)(DMF)_2Cl_3]$ (**3**), and $[Tb(dppz)(DMF)_2Cl_3]$ (**4**) have been structurally characterized from single-crystal X-ray diffraction study. They exhibit discrete neutral mononuclear species with the Eu^{3+} center in a ten coordinate $[EuN_2O_8]$ or $\{EuN_4O_6\}$ polyhedra for complexes **1** and **2** respectively and Tb^{3+} center in a seven-coordinate $\{TbN_2O_2Cl_3\}$ geometry for complexes **3** and **4**.

The $[Eu(dpq)(DMF)_2(NO_3)_3]$ (**1**) and $[Eu(dppz)_2(NO_3)_3]$ (**2**) crystallizes as $[Eu(dppz)_2(NO_3)_3]\cdot dppz\cdot Et_2O$ (**2·dppz·Et₂O**) in monoclinic space group $C2/c$, where in complex **1**, europium is ten-coordinated $\{EuN_2O_8\}$ geometry comprising of two nitrogen atoms of a bidentate dpq ligand, six oxygen atoms of three bidentate chelating nitrate ligands and two oxygen atoms of two DMF ligands. In complex **2** the europium center shows a ten-coordinate $\{EuN_4O_6\}$ coordination geometry originated from two bidentate *N,N'*-donor dppz ligands and three *O,O'*-donor bidentate nitrate ligands. The ORTEP diagrams of the complexes **1** and **2** are shown in Fig. 2. The ten-coordinate coordination polyhedron in complexes **1** and **2** could be best described closest to bicapped dodecahedron of non-crystallographic D_2 symmetry as concluded in analogous ten-coordinated $[La(bpy)_2(NO_3)_3]$ and $[La(phen)_2(NO_3)_3]$ complexes.[44] A 2-fold axis of symmetry, C_2 passes through Eu1, O4 and N4 in complex **1** and Eu1, O5 and N5 in complex **2**. The structure of complex **2** also contains one free dppz ligand and a diethyl ether as solvent of crystallization in the asymmetric unit introduced during it's crystal growth. The free dppz ligand is having strong favorable π-π stacking interactions (interplanar distance ~3.628 Å) with Eu-bound dppz in the three-dimensional crystal lattice (Fig. S5, ESI†). The Eu-O(NO_3) distances range from 2.492(4) Å to 2.547(4) Å for **1** and 2.495(3) Å to 2.504(4) Å for **2** respectively, The Eu-N and Eu-O(DMF) bond distances are 2.612(4) Å and 2.361(3) Å in complex **1**, while the Eu-N distances are in the range of 2.573(4) Å to 2.590(4) Å for **2**. Selected bond lengths and angles are given in Tables S2 and S3, ESI†. The unit cell packing diagrams for complexes **1** and **2**·dppz.Et_2O are given in supporting information (Fig. S5, ESI†).

$[Tb(dpq)(DMF)_2Cl_3]$ (**3**) and $[Tb(dppz)(DMF)_2Cl_3]$ (**4**) crystallizes in monoclinic space group $C2/c$ and triclinic space group $P\bar{1}$. The asymmetric units of the complexes contain one and two independent molecules. Each molecule contains one bidentate *N,N*-donor dpq or dppz ligand, two DMF molecules and three chloride ligands in a seven-coordinate $\{TbN_2O_2Cl_3\}$

coordination geometry. Such seven-coordinate polyhedron can be described as distorted mono-capped octahedron or distorted octahedral wedge geometry.[45] The Tb-N (dpq/dppz) bond distances in complexes are in the range of 2.572(2) to 2.630(2) Å in **3** and from 2.566(8) to 2.640(8) Å in **4** respectively. Tb-O(DMF) and Tb-Cl bond distances in complex **3** are in the range of 2.277(2) to 2.346(2) Å and 2.6338(8) to 2.6779(10) Å, whereas Tb-O(DMF) and Tb-Cl bond distances in complex **4** ranges from 2.244(6) to 2.378(6) Å and 2.632(3) to 2.673(3) Å respectively. The structural features of complexes **3** and **4** are essentially same due to identical ligand coordination around Tb^{3+}. The ORTEP views of the complexes **3** and **4** are shown in Fig. 3 and selected bond lengths and angles are shown in Tables S4 and S5 in ESI†. The unit cell packing diagrams for the complexes are given in Fig. S6 in ESI†. The coordination polyhedra of the respective lanthanide cores for the complexes **1**-**4** are shown in Fig. 4.

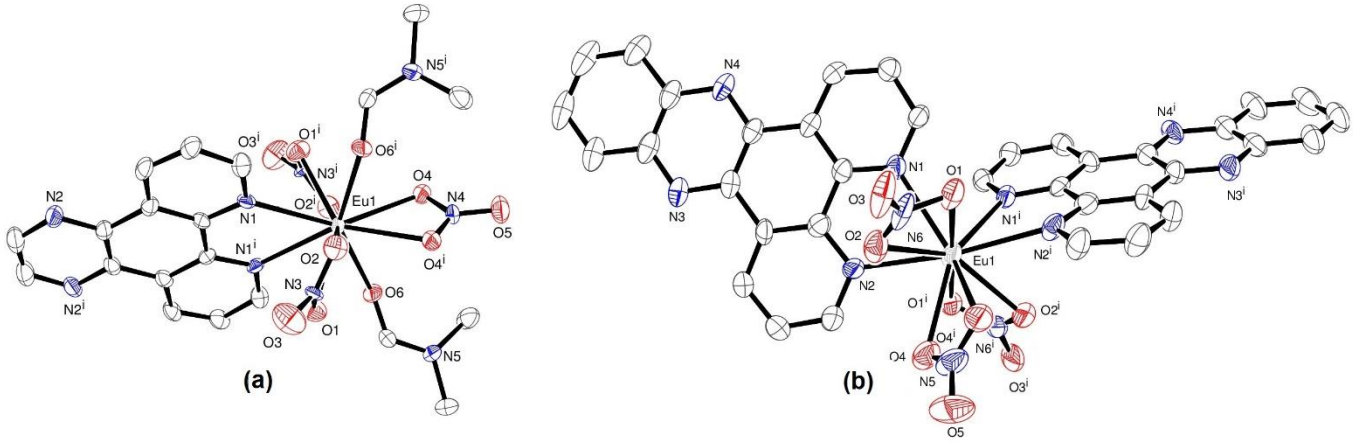

Fig. 2 An ORTEP view of (a) $[Eu(dpq)(DMF)_2(NO_3)_3]$ (**1**) and (b) $[Eu(dppz)(NO_3)_3]$ (**2**) in **2·dppz·Et₂O** showing 50% probability thermal ellipsoids and the atom numbering scheme for the metal and heteroatoms. The hydrogen atoms were omitted for clarity. Symmetry transformations used to generate equivalent atoms: For **1**, -x+1, y, -z+3/2; for **2** , -x+1, y, -z+1/2.

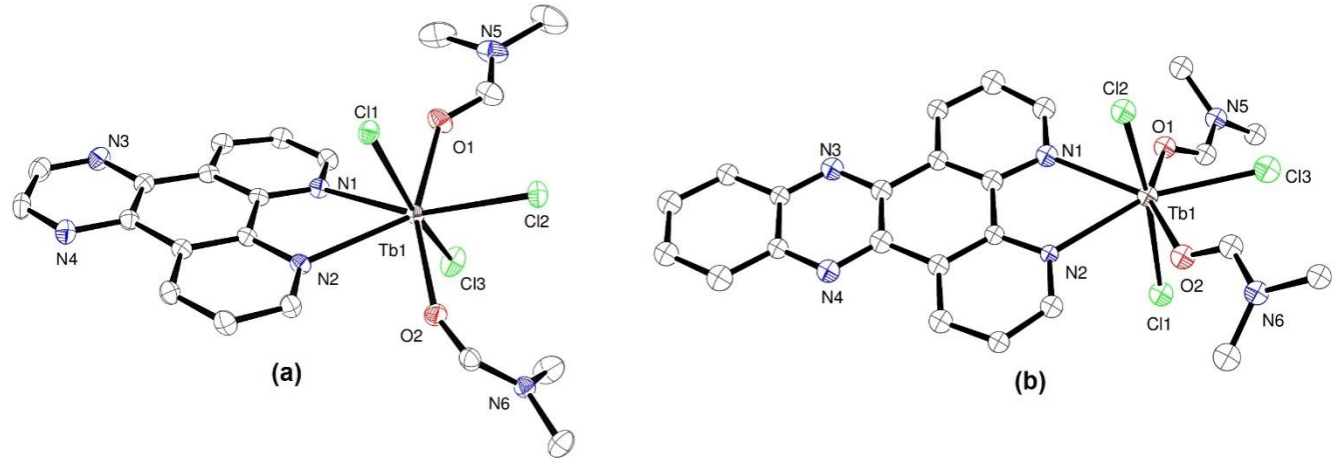

Fig. 3 An ORTEP view of (a) $[Tb(dpq)(DMF)_2Cl_3]$ (**3**) and (b) $[Tb(dppz)(DMF)_2Cl_3]$ (**4**) showing 50% probability thermal ellipsoids and the atom numbering scheme for the metal and heteroatoms. The hydrogen atoms were not shown for clarity.

DNA binding studies

Absorption spectral studies. DNA being one of the primary pharmacological target of the several metal-based therapeutic drugs like platins, thus studying DNA binding activities of metal complexes are of great importance towards designing and development of effective metallodrugs.[46] The binding propensity of the complexes **1**-**4** to CT-DNA was studied using various spectroscopic methods. The absorption spectral titration were carried out to determine the intrinsic binding constant (K_b) of the complexes to CT-DNA by monitoring the changes in absorption intensity of the complexes with increasing DNA concentrations (Fig. 5a, Figs. S15-S17, ESI†). Binding of complexes to DNA through intercalation generally results in hypochromism and bathochromic shift of absorption band due to strong stacking interaction between metal complexes and the DNA base pairs.[47] The intrinsic equilibrium binding constants (K_b) which gives a measure of strength of binding of a complex to CT-DNA are given in Table 1. The K_b values in the range of ~10^4 M^{-1} follow the order: **2**≈**4** (dppz)

>**1**≈**3** (dpq). The dppz complexes (**2**, **4**) show higher binding affinity compared to their dpq analogues (**1**, **3**) possibly due to

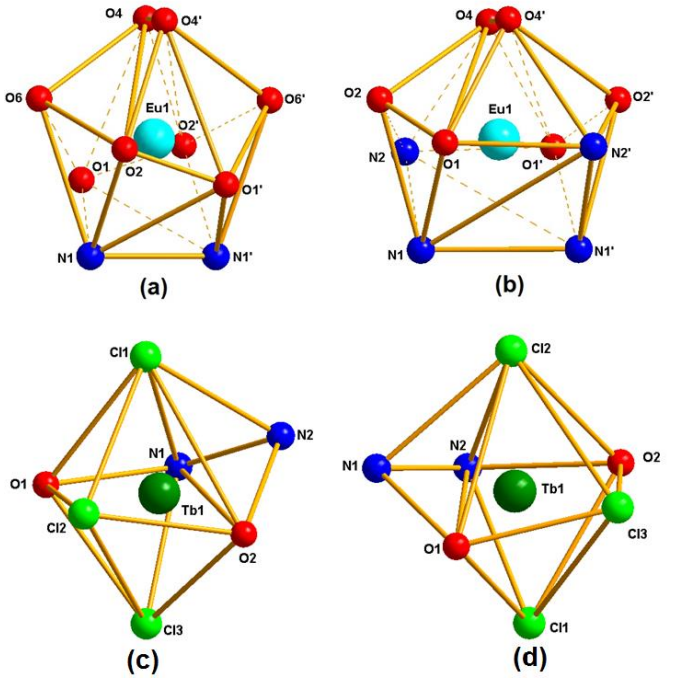

Fig. 4 Coordination polyhedra of the lanthanide cores for the complexes showing bicapped dodecahedron geometry in **1** (a) and **2** (b) and mono-capped octahedron geometry in **3** (c) and **4** (d).

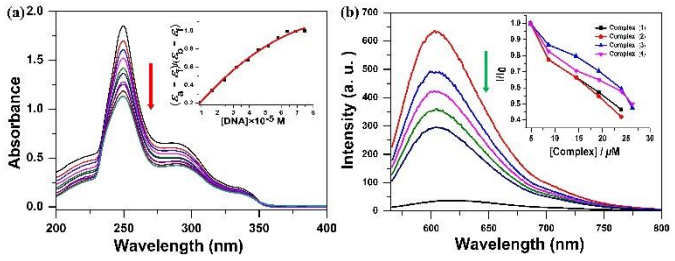

Fig. 5 (a) Absorption spectral traces of [Eu(dpq)(DMF)$_2$(NO$_3$)$_3$] (**1**) in 5 mM Tris-HCl/NaCl buffer (pH 7.2) with increasing CT-DNA concentration. The inset shows $\Delta\varepsilon_{af}/\Delta\varepsilon_{bf}$ *vs.* [DNA] plot for complex **1**. (b) Emission spectral traces of ethidium bromide bound CT-DNA with increasing concentration of complex **1** in 5 mM Tris-HCl/NaCl buffer medium (pH 7.2). The arrow shows the intensity changes on increasing the complex concentration. λ_{ex} = 546 nm, λ_{em} = 603 nm, [DNA] = 313 μM, [EthB] = 12 μM. The inset shows the plot of I/I_0 *vs.* [complex] for the complexes **1** (■), **2** (●), **3** (▲) and **4** (▼).

presence of an extended planar aromatic moiety in dppz which can intercalate strongly with the planar base pairs in DNA.

Ethidium bromide displacement assay. Ethidium bromide (EthB) displacement assay was used to determine the relative apparent binding constants (K_{app}) of the complexes **1**-**4** to CT-DNA (Table 1, Fig. 5b, Figs. S18-S20, ESI†). The K_{app} values of the complexes were measured by monitoring the progressive changes in emission intensity of ethidium bromide pretreated with CT-DNA as a function of increasing complex concentration.[48] Ethidium bromide acts as spectral probe as it exhibit enhanced emission intensity when intercalatively bound to DNA and reduced emission intensity in free state in buffer medium due to solvent quenching.[49] The competitive binding of the complexes to DNA could result in displacement of the bound EthB and solvent quenching and/or possible deformation of secondary DNA structure. The K_{app} values of the complexes were measured from the extent of reduction of EthB emission intensity by the complexes. The K_{app} values of the complexes are ~10^6 M^{-1} and follow the order of **2**≈**4** (dppz) >**1**≈**3**(dpq). Thus both K_b and K_{app} binding parameters suggest that studied Ln(dpq/dppz) complexes have good binding affinity to CT-DNA. The complexes are possibly DNA groove binders with dppz complexes showing a partial intercalative mode.

BSA binding studies

Serum albumin proteins constitute ~55% of total plasma proteins and play a crucial role in the drug transport and metabolism.[50] The binding affinity of complexes **1**-**4** with bovine serum albumin (BSA) were studied using intrinsic tryptophan emission quenching of BSA in presence of the complexes.[51] Upon gradual increase in concentration of the complexes **1**-**4**, the emission intensity of BSA at 345 nm decreases steadily (Fig. 6).

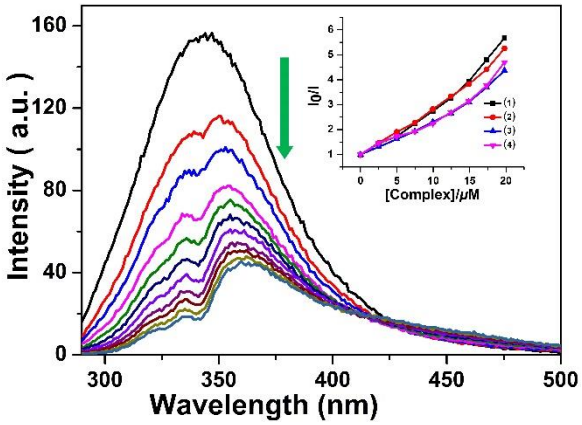

Fig. 6 The effect of addition of complex **1** on the fluorescence quenching of BSA in 5 mM Tris-HCl/NaCl buffer medium (pH 7.2). λ_{ex} = 295 nm, λ_{em} = 340 nm. The Inset shows the plot of I_0/I *vs.* [complex] for the complexes **1** (■), **2** (●), **3** (▲) and **4** (▼).

The quenching of emission can result from various molecular interactions arises due to changes in BSA secondary structure upon binding of the lanthanide complexes including subunit association, protein denaturation, substrate binding, or conformation changes of the protein.[52] The extent of the quenching of emission intensity is often measured from Stern-Volmer constant (K_{SV}), is considered to be a measure of the protein binding affinity of the complexes. The Stern-Volmer quenching constant (K_{BSA}) for complexes **1**-**4** have been calculated from slope of the linear plot of I_0/I vs. [complex] using Stern-Volmer equation[53,54] and corresponding values are listed in Table 1. Stern-Volmer plots are shown in supporting information (Fig. S21–S23, ESI†). The K_{BSA} values of ~10^4 M^{-1} indicate that the complexes favourably bind to serum proteins.

CT-DNA sensing application

The time-delayed luminescence measurements with emissive lanthanide complexes having sharp characteristic emission

bands, large Stokes shifts and long luminescence lifetimes have multiple advantages over organic fluorophores as luminescent probes for diverse applications in sensing and detection.[20-24] In these studies, a time delay is set between the excitation pulse and the detection window, thereby allowing the background autofluorescence to decay before measuring the luminescence of the probe. Lanthanide complexes with extremely long luminescence lifetimes in the millisecond range ideally suitable for such direct, time-gated detection of analyte in complex biological media.[29] The time-gated luminescence spectra of complexes **1**-**4** in the presence of increasing CT-DNA concentration were studied in Tris-HCl/NaCl buffer medium. The emission spectral changes of the complexes with increasing DNA concentration are shown in Fig. 7 and Figs. S24-S26 in ESI†.

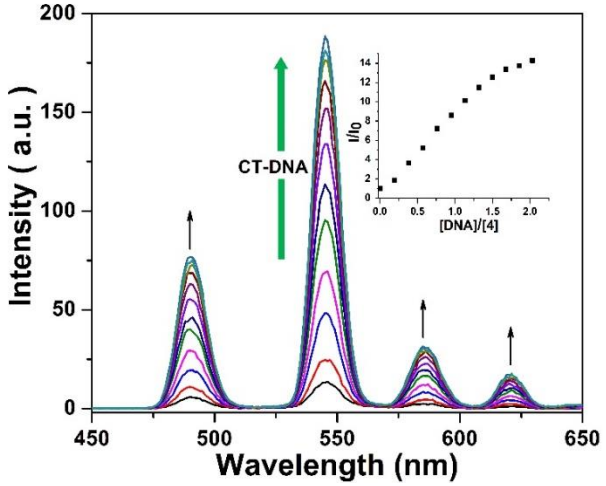

Fig. 7 The time-delayed luminescence spectra of $[Tb(dppz)(DMF)_2Cl_3]$ (**4**) (λ_{ex}= 272 nm) upon increasing concentration of CT-DNA in 5 mM Tris-HCl/NaCl (pH 7.2) medium at 298 K. Inset: relative emission intensity (I/I_0) *vs.* the [DNA]/[**4**] ratio.

Upon continuous addition of CT-DNA, the intensity of all the characteristic emission peaks for Eu^{3+} and Tb^{3+} are progressively increased. The most significant changes in emission intensity observed for the hypersensitive peak at 616 nm ($^5D_0 \rightarrow {}^7F_2$, ΔJ = 2) for Eu^{3+} complexes and at 545 nm ($^5D_4 \rightarrow {}^7F_5$, ΔJ = 1) for Tb^{3+} complexes respectively. We have observed a ~3-fold enhancement of emission intensity at 616 nm for Eu^{3+} complexes in presence of 2 equiv. of CT-DNA and ~14-fold enhancement at 545 nm for Tb^{3+} complex **4** in presence of 2 equiv. of CT-DNA (Inset, Fig. 7). The enhancement of emission intensity attributed to significant changes in inner coordination sphere of Ln^{3+} and thereby minimising the nonradiative quenching. In aqueous buffer medium water will replace the labile ligands like NO_3^-, Cl^- and DMF observed in solid state and thus quenches the emission by deactivating effect of vibrational quenching of O-H oscillators. When these complexes binds the DNA, bound water get displaced and thereby reduces nonradiative quenching and increases the emission intensity. This is proven through a series of Horrock's experiments[42] to determine the inner-sphere hydration number, *q*, the number of water molecules coordinated to the Ln^{3+} in solution, both in absence and presence of DNA. The results shows *q* ~4-6 in absence of DNA which is in agreement with dissociation of labile ligands and ligand exchange reactions with water. The appreciably lower hydration number (q < 1) in presence of DNA for complexes **1**-**4** reveals displacement of bound H_2O in a DNA-bound state, thus increase in emission intensity. DNA may occupy some of the inner sphere coordination sites of the Ln^{3+} ion through negatively charged oxygen atoms of phosphate and possibly N7 position of guanine.[55]

DNA photocleavage activity

The photo-induced DNA cleavage activities of the complexes **1**-**4** was studied using supercoiled (SC) pUC19 DNA (30 μM, 0.2 μg) in a medium of 50 mM Tris-HCl/NaCl buffer (pH 7.2) by irradiating the samples with a low power monochromatic UV-A light of 365 nm (6 W) (Fig. 8). The Eu^{3+} and Tb^{3+} complexes of respective photoactive dipyridoquinoxaline (dpq) and dipyridophenazine (dppz) ligands show significant DNA photocleavage activity through generation of photoexcited $^3(n\text{-}\pi^*)$ and/or $^3(\pi\text{-}\pi^*)$ states. The Eu^{3+} complexes **1** and **2** on photoexcitation at 365 nm for 2 h showed ~85% cleavage of supercoiled (SC) DNA to its nicked circular (NC) form at a complex concentration of 10 μM (lanes 10, 11 in Fig. 8). The Tb^{3+} complexes **3** and **4** showed essentially complete cleavage (≥ 90%) of SC DNA to its NC form under similar experimental conditions at 20 μM complex concentration (lanes 12, 13 in Fig. 8). The overall efficiency of reactive oxygen species generation is more favorable in complex **4** due to efficient ET to $^3O_2$ from low energy triplet excited state of dppz. The control experiments with only SC DNA did not show any apparent cleavage at 365 nm. The free dpq and dppz ligands showed only ~15% cleavage of SC DNA.

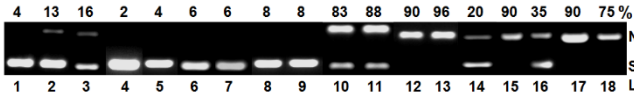

Fig. 8 Gel electrophoresis diagram showing the cleavage of SC pUC19 DNA (30 μM, 0.2 μg) by the complexes **1** – **4** in 50 mM Tris-HCl/NaCl buffer (pH, 7.2) on photo-irradiation with UV-A light of 365 nm (6 W) for 2 h: lane 1, DNA control; lane 2, DNA + dpq (10 μM); lane 3, DNA + dppz (10 μM); lane 4, DNA + $Eu(NO_3)_3{\cdot}6H_2O$ (10 μM); lane 5, DNA + $TbCl_3{\cdot}6H_2O$ (20 μM); lane 6, DNA + **1** (10 μM) (dark) ; lane 7, DNA + **2** (10 μM) (dark); lane 8, DNA + **3** (20 μM) (dark); lane 9, DNA + **4** (20 μM) (dark); lane 10, DNA + **1** (10 μM); lane 11, DNA + **2** (10 μM); lane 12, DNA + **3** (20 μM); lane 13, DNA + **4** (20 μM); lane 14, DNA + methyl green (200 μM); Lane 15, DNA + methyl green (200 μM) + **1** (10 μM); Lane 16, DNA + methyl green (200 μM) + **2** (10 μM); lane 17, DNA + methyl green (200 μM) + **3** (20 μM); Lane 18, DNA + methyl green (200 μM) + **4** (20 μM).

This observation is in conformity with the photosensitizing ability of dpq and dppz ligands. The extent of photocleavage of SC DNA to NC form increases with increasing concentration of the complexes and exposure time (Figs. S27-S29 in ESI†). Control experiments performed with only SC DNA or with metal salts do not show any apparent photocleavage of DNA. The complexes were cleavage inactive in dark condition, thus ruling out possibility of any hydrolytic DNA cleavage (lanes 6-9 in Fig. 8). The DNA groove binding preferences of the complexes were studied using DNA major groove binder methyl green (Fig. 8). Methyl green alone showed moderate ~20% cleavage of SC-DNA on exposure to UV-A light due to its photosensitizing ability. Methyl green pretreated SC DNA with dppz complexes show significant inhibition of photocleavage activity. The dpq

complexes display no apparent inhibition of photocleavage activity in presence of methyl green. This data suggest minor groove binding preference for the dpq (**1** and **3**) and major groove binding preference for the dppz (**2** and **4**) complexes respectively.[4]

Mechanistic studies. The mechanistic aspects of the DNA photocleavage reactions of the complexes **1**-**4** have been studied in the presence of various additives (Fig. 9, and Figs. S30, S31 in ESI†). A series of control experiments were carried out using reagents like sodium azide and L-histidine as singlet oxygen quenchers[56] and DMSO, catalase and KI as hydroxyl radical scavengers.[57,58] Addition of singlet oxygen quenchers like NaN_3 and L-histidine partially inhibits the photo-induced DNA cleavage activity, whereas hydroxyl radical scavengers like DMSO, KI or catalase also show moderate inhibition in photo-induced DNA cleavage. The formation of $^1O_2$ is also evidenced from the enhanced photocleavage activity in D_2O because of longer lifetime of $^1O_2$ than that in water.[59] These results is suggestive towards involvement of both $^1O_2$ and $^\bullet OH$ radicals as cleavage active reactive oxygen species involving both type-II and photoredox pathways respectively and in conformity with earlier reports from analogous lanthanide complexes.[36-39]

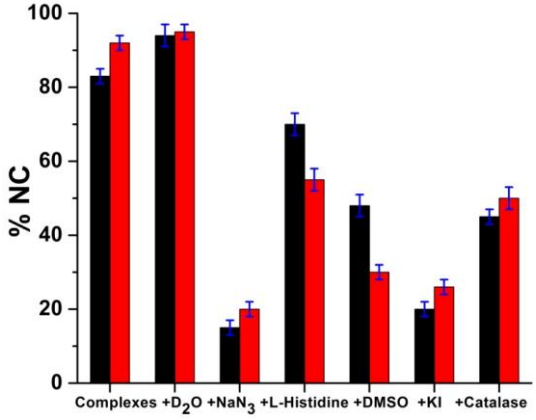

Fig. 9 Cleavage of SC pUC19 DNA (30 μM, 0.2 μg) by complex **1** (10 μM) (black) and complex **3** (20 μM) (red) on photoexposure at 365 nm (6 W) for 2 h in the presence of various additives in Tris-HCl/NaCl buffer. The additive concentrations/quantities are NaN_3, 0.2 mM; KI, 0.2 mM; D_2O, 16 μL; L-histidine, 0.2 mM; DMSO, 4 μL; catalase, 4 units.

Experimental

Materials and methods

1,10-phenanthroline (phen), 1,2-diaminobenzene, ethylene diamine and $TbCl_3{\cdot}6H_2O$ and Eu_2O_3 were purchased from Sigma-Aldrich and used without further purification. Solvents used were of analytical or spectroscopic grade purchased from commercial sources or purified by standard procedure.[60] $Eu(NO_3)_3{\cdot}5H_2O$ prepared by digesting anhydrous Eu_2O_3 (99.99%) with diluted nitric acid. Supercoiled (SC) plasmid pUC19 (CsCl purified) was purchased from Merck Millipore. Tris-(hydroxymethyl)-aminomethane-HCl (Tris-HCl) buffer solution was prepared using Milli-Q water (18.2 MΩ). Calf thymus (CT) DNA, Bovine serum albumin (BSA, fraction V), agarose (molecular biology grade), methyl green, catalase, ethidium bromide (EthB), gel loading solution (containing 0.25% (w/v) bromophenol blue, 0.25% Xylene cyanole FF and 40% sucrose in water) were from Sigma (U.S.A.). dipyrido-[3,2-d:2′,3′-f]-quinoxaline (dpq) and dipyrido[3,2-a:2′,3′-c]phenazine (dppz) were prepared according to known literature procedure using 1,10-phenanthroline-5,6-dione as a precursor reacted with ethylenediamine for dpq and 1,2-phenylenediamine for dppz ligand.[61,62] The elemental microanalyses were performed on a Perkin-Elmer model Perkin-Elmer 2400 Series-II elemental analyzer instrument. The infrared spectra were recorded on a Perkin-Elmer model 1320 FT-IR spectrometer in KBr pellets in the 4000-400 cm^{-1} range. Electronic spectra were recorded at 298 K on a Varian V670 and Perkin-Elmer Lambda 25 spectrophotometers. Electrospray ionization mass spectral (ESI-MS) measurements were carried out using a WATERS Q-TOF Premier mass spectrometer. The fluorescence and time-delayed luminescence spectra at 298 K were obtained using an Agilent Cary Eclipse fluorescence spectrophotometer. Lifetime measurements for complexes **1**-**4** were performed under ambient conditions in DMF, H_2O and D_2O using a pulsed Xenon lamp at λ_{ex} = 272 nm and λ_{em} = 616 nm and 545 nm for Eu^{3+} and Tb^{3+} complexes respectively with a delay time and gate time of 0.1 ms. Decay curves were fitted by non-linear least square method. Excited state lifetime measurements of complexes **1**-**4** in the presence of CT-DNA (50 μM) were measured in 5 mM Tris-HCl/NaCl buffer (pH 7.2) containing 2% DMF prepared in Milli-Q water and in D_2O. Data acquisition and analysis was performed by the aforementioned procedure. Lifetime data for **1–4** complexes under various conditions were shown in Figures S12-S14, Tables S6, S7, ESI†). To check the oxygen sensitivity of $[Tb(dppz)(DMF)_2Cl_3]$ (**4**), Luminescence lifetime measurements were carried out in aerated and degassed aqueous solution after thorough sparging with dioxygen-free nitrogen.

The excited state lifetime measurements in water and deuterium oxide allowed the determination of the number of water molecules (q) directly coordinated to the respective lanthanide center in complexes **1**-**4** using the following modified Horrocks' equations for Eu^{3+} and Tb^{3+} respectively.[42]

$$q_{Eu} = 1.2\left(\frac{1}{\tau_{H_2O}} - \frac{1}{\tau_{D_2O}} - 0.25\right)$$

$$q_{Tb} = 5.0\left(\frac{1}{\tau_{H_2O}} - \frac{1}{\tau_{D_2O}} - 0.06\right)$$

The overall luminescence quantum yields of the complexes were measured at 298 K according to a reported procedure using quinine sulfate as reference using following equation:[53]

$$\emptyset_{overall} = \emptyset_{ref}\frac{A_{ref}In^2}{AI_{ref}n_{ref}^2}$$

where A, I and n denote the respective absorbance at the excitation wavelength, area under the emission spectral curve and refractive index of the solvent respectively. The ϕ_{ref} represents the quantum yield of the standard quinine sulfate solution. Electrochemical measurements were made on a CH

Instruments Model CHI 610E potentiostat with electrochemical analysis software using a three-electrode setup consist of a glassy carbon working, platinum wire auxiliary, and Ag/AgCl reference electrode. Tetrabutylammonium perchlorate (TBAP, 0.1 M) was used as a supporting electrolyte in DMF.

Synthesis and characterization

Synthesis of $[Eu(dpq)(NO_3)_3(DMF)_2]$ (1), $[Eu(dppz)_2(NO_3)_3]$ (2), $[Tb(dpq)(DMF)_2Cl_3]$ (3) and $[Tb(dppz)(DMF)_2Cl_3]$ (4).

The complexes **1**-**4** were prepared by following a generalized synthetic procedure in which a hot methanolic solution of $Eu(NO_3)_3{\cdot}5H_2O$ (0.200 g; 0.467 mmol) and $TbCl_3{\cdot}6H_2O$ (0.200 g; 0.535 mmol) in boiling methanol (10 mL) was added dropwise to a hot stirred methanolic solution (20 mL) of the respective heterocyclic bases (dpq/dppz) [0.108 g dpq, 0.467 mmol (**1**); 0.263 g dppz; 0.934 mmol (**2**); 0.124 g dpq, 0.535 mmol (**3**) and 0.151 g dppz, 0.535 mmol (**4**)]. The resulting mixture was stirred for 2 h in water bath at 60 ^{0}C to obtain a precipitate which was filtered and successively washed with hot methanol (2 x 5 mL), diethyl ether (2 x 5 mL), and finally dried in vacuum over P_4O_{10} [Yield: ~80%]. On layering of the compounds dissolved in DMF with diethyl ether at RT, block shaped yellow to brown crystals were obtained suitable for X-ray crystallography. The characterization data for the complexes are given below.

$[Eu(dpq)(DMF)_2(NO_3)_3]$ (1). Yield: 0.268 g (80%). Anal. calc. for $C_{20}H_{22}N_9O_{11}Eu$: C, 33.53; H, 3.10; N, 17.60. Found: C, 33.38; H, 3.04; N, 17.58. ESI-MS (DMF): *m/z* 719.21 $[M+H]^+$. Calcd: *m/z* 719.07. FT-IR (KBr, cm^{-1}): 3387(w, br), 3093(w), 1607(s), 1580(s), 1533(s), 1495(s), 1470(s), 1406(s), 1394(vs, NO_3^-), 1307(m), 1288(s), 1214(m), 1056(s), 838(s), 817(m) (vs, very strong; s, strong; m, medium; w, weak; br, broad). UV-visible in DMF [λ, nm (ε, $M^{-1}cm^{-1}$)]: 273 (77360). Molar conductance in aqueous DMF (1:9) at 298 K (Λ_M): 102 S cm^2 M^{-1}.

$[Eu(dppz)_2(NO_3)_3]$ (2). Yield: 0.282 g (81%). Anal. calc. for $C_{36}H_{20}N_{11}O_9Eu$: C, 47.91; H, 2.23; N, 17.07. Found: C, 48.11; H, 2.76; N, 17.02. ESI-MS (in DMF-EtOH): *m/z* 949.19 ($[M+C_2H_5OH]^+$, 100%). Calcd: *m/z* 949.11. FT-IR (KBr, cm^{-1}): 3395(w, br), 3092(w), 1601(s), 1577(m), 1497(s), 1419(s), 1385(s), 1363(s), 1310(m), 1230(s), 1187(m), 1136(s), 1045(s), 843(s), 821(s). UV-visible in DMF [λ, nm (ε, $M^{-1}cm^{-1}$)]: 376sh (28970), 365 (29000), 272 (98180). Molar conductance in aqueous DMF (1:9) at 298 K (Λ_M): 122 S cm^2 M^{-1}.

$[Tb(dpq)(DMF)_2Cl_3]$ (3). Yield: 0.288 g (80%). Anal. calc. for $C_{20}H_{22}N_6O_2Cl_3Tb$: C, 37.32; H, 3.44; N, 13.06. Found: C, 37.21; H, 3.36; N, 13.03. ESI-MS (in DMF-MeOH): *m/z* 676.45 $[M+MeOH]^+$, calcd: *m/z* 676.05, FT-IR (KBr, cm^{-1}): 3336 (w, br), 1636 (w), 1581(s), 1530(s), 1472(m), 1390(s), 1212(m), 1119(s), 1081(s), 810(s), 737 (s), 701(s). UV-visible in DMF [λ, nm (ε, $M^{-1}cm^{-1}$)]: 273 (75650). Molar conductance in aqueous DMF (1:9) at 298 K (Λ_M): 82 S cm^2 M^{-1}.

$[Tb(dppz)(DMF)_2Cl_3]$ (4). Yield: 0.293 g (79%). Anal. calc. for $C_{24}H_{24}N_6O_2Cl_3Tb$: C, 41.55; H, 3.49; N, 12.11. Found: C, 41.49; H, 3.63; N, 12.10. ESI-MS (in DMF): *m/z* 694.30 $[M+H]^+$, calcd: *m/z* 694.04. FT-IR (KBr, cm^{-1}): 3242 (w, br), 1632(w), 1578(m), 1492(s), 1465(s), 1416(m), 1363(s), 1337(s), 1230(m), 1135(s), 1077(s), 1044(s), 814(s), 762(s), 738(s), 701(s), 636(s). UV-visible in DMF [λ, nm (ε, $M^{-1}cm^{-1}$)]: 376sh (27650), 365 (27680), 272 (93180). Molar conductance in aqueous DMF (1:9) at 298 K (Λ_M): 89 S cm^2 M^{-1}.

Single-Crystal X-ray Structure Determination

Complexes **1**-**4** were structurally characterized by single-crystal X-ray diffraction technique. Single crystals of suitable dimensions were mounted on a glass fiber and used for data collection. All geometric and intensity data were collected on a Bruker D8 Quest Microfocus X-Ray CCD diffractometer equipped with an Oxford Instruments low-temperature attachment, with graphite-monochromated Mo Kα radiation (λ = 0.71073 A˚) at 100(2) K using ω-scan technique (width of 0.5° per frame) at a scan speed of 10 s per frame controlled by manufacturer's APEX2 v2012.4-3 software package.[63] Intensity data, collected using ω-2θ scan mode, were corrected for Lorentz-polarization effects,[64] processed and integrated with Bruker's SAINT software. Multiscan absorption corrections were applied with the SADABS program.[65] The space group was determined using XPREP. The structures were subsequently solved by the direct methods using SHELXS-97[66] and was refined on F^2 by full-matrix least-squares technique using the SHELXTL 6.14 software package.[67] The structures were further refined and processed with the SHELXL-97 incorporated into the WinGX 1.70 crystallographic package.[68] All non-hydrogen atoms were refined anisotropically till convergence is reached. All the hydrogen atoms were included in idealized positions and refined using a riding model. Selected crystallographic data and refinement parameters for complexes **1**-**4** are summarized in Table S1. Selected bond distances and angles for all the complexes are given in Tables S2-S5. Perspective views of the complexes were obtained using ORTEP.[69] The CCDC deposition numbers for the complexes **1**-**4** are 1402312-1402315 respectively. Copies of this information can be obtained free of charge upon application to CCDC, 12 Union Road, Cambridge CB21EZ, U.K.

DNA binding experiments

Calf thymus (CT) DNA in Tris-HCl/NaCl buffer (5 mM Tris-HCl, 5 mM NaCl in water, pH 7.2) gave a ratio of UV absorbance at 260 and 280 nm, A_{260}/ A_{280} of 1.8-1.9, indicating that DNA is apparently free from protein.[70] Concentrated stock solutions of CT-DNA were prepared in this buffer with sonication. The concentration of CT-DNA was determined from its absorbance intensity at 260 nm with a known molar extinction coefficient (ε_{260}) of 6600 $M^{-1}cm^{-1}$.[71] Solutions of metal complexes were prepared in DMF and quantitatively diluted to the required concentration for DNA binding experiments. Absorption spectral titration experiments were made on a UV-visible spectrophotometer by varying the concentration of the CT-DNA while maintaining a constant metal complex concentration. Due corrections was made for the absorbance of CT DNA itself. Spectra were recorded after equilibration of the sample for 5 min. The intrinsic equilibrium DNA binding constant (K_b) of the lanthanide complexes **1**-**4** was obtained using the equation

$$[DNA]/(\varepsilon_a-\varepsilon_f) = [DNA]/(\varepsilon_b-\varepsilon_f) + 1/K_b(\varepsilon_a-\varepsilon_f)$$

Where [DNA] is the concentration of DNA in the base pairs, ε_a is the apparent extinction coefficient observed for the complex, ε_f

corresponds to the extinction coefficient of the complex in its free form, and ε_b refers to the extinction coefficient of the complex when fully bound to DNA.[72] Data were plotted using Origin Lab, version 8.0 to obtain the [DNA]/($\varepsilon_a-\varepsilon_f$) vs. [DNA] linear plots. The ratio of the slope to intercept from the linear fit gives the value of the intrinsic binding constant (K_b).

The competitive binding assay from ethidium bromide (EthB) displacement were carried out in 5 mM Tris-HCl/NaCl buffer (pH 7.2) by measuring emission intensities of a EthB bound CT DNA solution with gradual increment of complex concentrations. The emission intensities of EthB at 603 nm (λ_{ex} = 546 nm) were recorded after each addition of the complex. EthB showed no apparent emission in Tris-buffer medium because of fluorescence quenching of free ethidium bromide by solvent molecules. CT DNA bound EthB showed significantly enhanced fluorescence intensity. The apparent binding constants (K_{app}) values were obtained from the equation: K_{app} x C_{50} = K_{EthB} x [EthB], where K_{app} is the apparent binding constant of the complex studied, C_{50} is the concentration of the complex at 50% quenching of DNA-bound ethidium bromide emission intensity, K_{EthB} is the binding constant of the ethidium bromide (K_{EthB} = 1 x 10^7 M^{-1}), and [EthB] is the concentration of ethidium bromide (12 μM).[73]

Protein binding experiments

The interaction of the complexes **1-4** with bovine serum albumin (BSA) has been studied from tryptophan emission-quenching experiments. The complex solutions were gradually added to the solution of BSA (5 μM) in 5 mM Tris-HCl-NaCl buffer (pH 7.2) and the quenching of the emission signals at 340 nm (λ_{ex} = 295 nm) were recorded. The quenching constant (K_{BSA}) has been determined quantitatively by using Stern-Volmer equation.[53] Stern-Volmer plots for I_0/I vs. [complex] were made using the corrected fluorescence data taking into account the effect of dilution. Linear fit of the data using the equation: $I_0/I = 1 + K_{BSA}$ [Q], where I_0 and I are the emission intensities of BSA in the absence of quencher and in the presence of quencher of concentration [Q], gave the quenching constants (K_{BSA}).[54]

DNA cleavage experiments

The cleavage of plasmid supercoiled (SC) pUC19 (30 μM, 0.2 μg, 2686 base pairs) was performed by agarose gel electrophoresis in Tris-Acetate-EDTA (TAE) buffer (pH 8.1) by treating DNA with varying concentration of complexes **1**-**4** in the absence of any additives. The concentration of the complexes in DMF or the additives in buffer corresponds to the values after dilution to 20 μL final volume using 50 mM Tris-HCl/NaCl buffer (pH 7.2). Photo-induced DNA cleavage reactions were carried out in a dark room at 25 ^{0}C under illuminated conditions using UV-A light of 365 nm (6 W, Model VL-6.LC from Vilber Lourmat, France). The solution path length in the sample vial was 5 mm. After photo-exposure, each sample was incubated for 1.0 h at 37 °C and analyzed for the photocleaved DNA fragments using gel electrophoresis. Mechanistic studies were carried out using different additives or radical scavenging agents, viz. DMSO, NaN_3, L-Histidine, KI, catalase, D_2O to SC DNA prior the addition of the complexes. To the treated DNA samples after incubation in a dark chamber 3 μL of loading buffer (0.25% bromophenol blue, 0.25% xylene cyanol, and 40% sucrose) was added. The sample was then loaded on 1% agarose gel containing 1.0 μg/mL ethidium bromide an electrophoresed for 2.0 h at 60 V in TAE gel running buffer. After electrophoresis, the bands were visualized by UV-A light and photographed using UVITEC FireReader V4 gel documentation system. Quantification of cleavage products was performed by measuring the intensities of the bands using the UVIBand software. Supercoiled plasmid DNA values were corrected for lower binding affinity of ethidium bromide to SC DNA compared to nicked circular (NC) or linear form of DNA.[74] The error observed in measuring the band intensities were in the range of 4-6%.

Conclusions

In conclusion, a new series of luminescent europium and terbium complexes having *N*,*N*-donor phenanthroline bases have been synthesized and structurally characterized. The Eu^{3+} complexes showed ten-coordinate $\{EuN_2O_8\}$ or $\{EuN_4O_6\}$ core with bicapped dodecahedron geometry and Tb^{3+} complexes showed seven coordinate $\{TbN_2O_2Cl_3\}$ core with distorted mono-capped octahedral structure. The complexes showed good DNA and protein binding propensity in aqueous buffer medium through groove binding and partial intercalation from planar dpq/dppz bases. Time-gated luminescence studies showed significant enhancement of emission intensity in presence of DNA due to reduction in the number of coordinated water molecules that causes excited state quenching by energy transfer to O-H oscillators. The complexes **1**-**4** displayed efficient photo-induced DNA cleavage activity at low power UV-A light of 365 nm following singlet oxygen and hydroxyl radical in a photoredox pathway at micromolar concentration. Here dpq and dppz ligands act as efficient light harvesting antenna moiety which upon photoexcitation showed efficient energy transfer to populate long-lived luminescent excited states of Eu^{3+} and Tb^{3+} for *f-f* transition alongwith generation of reactive oxygen species involved in DNA damage activity. Further studies are on to design stable highly luminescent multimodal bioresponsive lanthanide complexes for chemotherapeutic and diagnostic applications.

Acknowledgements

We thank IIT Kanpur for startup grant and Science and Engineering Research Board (SERB), Government of India, (SB/FT/CS-062/2012) for financial support. S.D. thank IIT Kanpur and Ministry of Human Resource Development (MHRD) for research fellowship.

Notes and references

1 (a) D. S. Sigman, A. Mazumdar and D. M. Perrin, *Chem. Rev.,* 1993, **93**, 2295-2316; (b) D. S. Sigman, T. W. Bruice, A. Mazumdar, and C. L. Sutton, *Acc. Chem. Res.,* 1993, **26**, 98-104.

2 (a) H. T. Chifotides and K. R. Dunbar, *Acc. Chem. Res*., 2005, **38**, 146-156; (b) P. M. Bradley, A. M. Angeles-Boza, K. R. Dunbar and C. Turro, *Inorg. Chem.*, 2004, **43**, 2450-2452.
3 (a) C. J. Burrows and J. G. Muller, *Chem. Rev.*, 1998, **98**, 1109-1151; (b) B. Meunier, *Chem. Rev.*, 1992, **92**, 1411-1456.
4 K. E. Erkkila, D. T, Odom and J. K. Barton, *Chem. Rev*., 1999, **99**, 2777-2795.
5 (a) W. K. Pogozelski and T. D. Tullius, *Chem. Rev.*, 1998, **98** 1089-1107; (b) B. Armitage, *Chem. Rev.,* 1998, **98**, 1171-1200; (c) D. R. McMillin and K.M. McNett, *Chem. Rev.*, 1998, **98**, 1201-1219; (d) C. Metcalfe and J. A. Thomas, *Chem. Soc. Rev.*, 2003, **32**, 215-224.
6 N. P. E. Barry and P. J. Sadler, *Chem. Commun.*, 2013, **49**, 5106-5131.
7 (a) E. R. Jamieson and S. J. Lippard, *Chem. Rev.,* 1999, **99**, 2467-2498; (b) T. C. Johnstone, J. J. Wilson and S. J. Lippard, *Inorg. Chem*., 2013, **52**, 12234-12249.
8 P. C. A. Bruijnincx and P. J. Sadler, *Curr. Opin. Chem. Biol*., 2008, **12**, 197-206.
9 (a) S. Dhar, D. Senapati, P. A. N. Reddy, P. K. Das and A. R. Chakravarty, *Chem. Commun.*, 2003, 2452-2453; (b) S. Dhar, D. Senapati, P. K. Das, P. Chattopadhyay, M. Nethaji and A. R. Chakravarty, *J. Am. Chem. Soc.,* 2003, **125**, 12118-12124.
10 (a) G. Gasser and N. Metzler-Nolte, *Curr. Opinion Chem. Biol.*, 2012, **16**, 84-91; (b) G. Gasser, I. Ott and N. Metzler-Nolte, *J. Med. Chem.*, 2011, **54**, 3-25.
11 R. Bonnett, *Chemical Aspects of Photodynamic Therapy*, Gordon & Breach: London, U. K., 2000.
12 (a) M. R. Detty, S. L. Gibson and S. J. Wagner, *J. Med. Chem.*, 2004, **47**, 3897-3915; (b) M. Triesscheijn, P. Baas, J. H. M. Schellens and F. A. Stewart, *Oncologist*, 2006, **11**, 1034-1044; (c) M. Ethirajan, Y. Chen, P. Joshi and R. K. Pandey, *Chem. Soc. Rev*., 2011, **40**, 340-362.
13 (a) M. H. Lim, H. Song, E. D. Olmon, E. E. Dervan and J. K. Barton, *Inorg. Chem.*, 2009, **48**, 5392-5397; (b) A. Sitlani, E. C. Long, A. M. Pyle and J. K. Barton, *J. Am. Chem. Soc.*, 1992, **114**, 2303-2312.
14 K. Szaciłowski, W. Macyk, A. Drzewiecka-Matuszek, M. Brindell and M. Stochel, *Chem. Rev.*, 2005, **105**, 2647-2694.
15 (a) E. D. Stenberg, D. Dolphin and C. Brückner, *Tetrahedron*, 1998, **54**, 4151-4202; (b) M. C. DeRosa and R. J. Crutchley, *Coord. Chem. Rev*., 2002, **233/4**, 351-371.
16 H. Ali and J. E. van Lier, *Chem. Rev*., 1999, **99**, 2379-2450.
17 M. Kar and A. Basak, *Chem. Rev.*, 2007, **107**, 2861-2890.
18 (a) P. Caravan, J. J. Ellison, T. J. McMurry and R. B. Lauffer, *Chem. Rev.*, 1999, **99**, 2293-2352; (b) P. Caravan, *Chem. Soc. Rev*., 2006, **35**, 512-523; (c) E. Boros, E. M. Gale and P. Caravan, *Dalton Trans.*, 2015, **44**, 4804-4818.
19 (a) M. Bottrill, L. Kwok and N. J. Long, *Chem. Soc. Rev.*, 2006, **35**, 557-571; (b) E. J. Werner, A. Datta, C. J. Jocher and K. N. Raymond, *Angew. Chem. Int. Ed*., 2008, **47**, 8568-8580; (c) E. Debroye and T. N. Parac-Vogt, *Chem. Soc. Rev*., 2014, **43**, 8178-8192.
20 (a) J.-C. G. Bünzli and C. Piguet, *Chem. Soc. Rev.*, 2005, **34**, 1048-1077; (b) J.-C. G. Bünzli, *Chem. Rev.*, 2010, **110**, 2729-2755.
21 M. C. Hefferin, L. M. Matosziuk and T. J. Meade, *Chem. Rev*., 2014, **114**, 4496-4539.
22 (a) C. P. Montgomery, B. S. Murray, E. J. New, R. Pal and D. Parker, *Acc. Chem. Res.,* 2009, **42**, 925-937; (b) J. Yu, D. Parker, R. Pal, R. A. Poole and M. J. Cann, *J. Am. Chem. Soc*., 2006, **128**, 2294-2299; (c) S. J. Butler, L. Lamarque, R. Pal and D. Parker, *Chem. Sci.*, 2014, **5**, 1750-1756.
23 (a) T. Gunnlaugsson and J. P. Leonard, *Chem. Commun*., 2005, 3114-3131; (b) T. Gunnlaugsson and F. Stomeo, *Org. Biomol. Chem*., 2007, **5**, 1999-2009.
24 E. G. Moore, A. P. S. Samuel and K. N. Raymond, *Acc. Chem. Res.,* 2009, **42**, 542-552.
25 (a) B. K. Takasaki and J. Chin, *J. Am. Chem. Soc.*, 1994, **116**, 1121-1122; (b) J. Sumaoka, Y. Azuma and M. Komiyama, *Chem. Eur. J.*, 1998, **4**, 205-209; (c) M. Komiyama, N. Takeda and H. Shigekawa, *Chem. Commun.*, 1999, 1443-1451; (d) S. J. Franklin, *Curr. Opin. Chem. Biol.*, 2001, **5**, 201-208.
26 (a) M. E. Branum, A. K. Tipton, S. Zhu and L. Que, Jr. *J. Am. Chem. Soc.*, 2001, **123**, 1898-1904; (b) M. E. Branum and L. Que, Jr. *J. Inorg. Biochem.,* 1999, **4**, 593-600.
27 (a) A. Roigk, R. Hettich and H. –J. Schneider, *Inorg. Chem.*, 1998, **37**, 751-756; (b) J. Rammo, R. Hettich, A. Roigk and H. -J. Schneider, *Chem. Commun*., 1996, 105-107.
28 (a) M. A. Camargo, A. Neves, A. J. Bortoluzzi, B. Szpoganicz, F. L. Fischer, H. Terenzi, O. A. Serra, V. G. Santos, B. G. Vaz and M. N. Eberlin, *Inorg. Chem.,* 2010, **49**, 6013-6025; (b) C. A. Chang, B. H. Wu and B. Y. Kuan, *Inorg. Chem.,* 2005, **44**, 6646-6654.
29 (a) A. Thibon and V. C. Pierre, *Anal. Bioanal. Chem*., 2009, **394**, 107-120; (b) K. Hanaoka, K. Kikuchi, S. Kobayashi and T. Nagano, *J. Am. Chem. Soc.*, 2007, **129**, 13502-13509.
30 M. H. Lim, H. Song, E. D. Olmon, E. E. Dervan and J. K. Barton, *Inorg. Chem.*, 2009, **48**, 5392-5397.
31 (a) H. T. Chifotides and K. R. Dunbar, *Acc. Chem. Res.*, 2005, **38**, 146-156; (b) S. L. H. Higgins and K. J. Brewer, *Angew. Chem. Int. Ed*., 2012, **51**, 11420-11422.
32 (a) N. J. Farrer, L. Salassa and P. J. Sadler, *Dalton Trans*., 2009, 10690-10701; (b) J. S. Butler, J. A. Woods, N. J. Farrer, M. E. Newton and P. J. Sadler, *J. Am. Chem. Soc.,* 2012, **134**, 16508−16511.
33 (a) A. K. Patra, T. Bhowmick, S. Roy, S. Ramakumar and A. R. Chakravarty, *Inorg. Chem*., 2009, **48**, 2932-2943; (b) A. K. Patra, T. Bhowmick, S. Ramakumar, M. Nethaji and A. R. Chakravarty, *Dalton Trans*., 2008, 6966-6976; (c) A. K. Patra, M. Nethaji and A. R. Chakravarty, *Dalton Trans*., 2005, 2798-2804.
34 (a) K. Mitra, S. Patil, P. Kondaiah and A. R. Chakravarty, *Inorg. Chem*., 2015, **54**, 253-264; (b) S. Banerjee, A. Dixit, R. N. Sridharan, A. A. Karande and A. R. Chakravarty, *Chem. Commun*., 2014, **50**, 5590-5592; (c) U. Basu, I. Pant, I. Khan, A. Hussain, P. Kondaiah and A. R. Chakravarty, *Angew. Chem. Int. Ed.,* 2012, **51**, 2658-2661.
35 (a) B. A. Albani, B. Peña, N. A. Leed, N. A. B. G. de Paula, C. Pavani, M. S. Baptista, K. R. Dunbar and C.Turro*, J. Am. Chem. Soc.*, 2014, **136**, 17095-17101; (b) B. Peña, A. David, C. Pavani, M. S. Baptista, J.-P. Pellois, C. Turro and K. R. Dunbar, *Organometallics*, 2014, **33**, 1100-1103.
36 (a) S. W. Young, K. W. Woodburn, M. Wright, T. D. Mody, Q. Fan, J. L. Sessler, W. C. Dow and R. A. Miller, *Photochem. Photobiol*., 1996, **63**, 892-897; (b) J. L. Sessler and R. A. Miller, *Biochem. Pharmacol.*, 2000, **59**, 733-739.
37 (a) G.-J. Chen, X. Qiao, J.-L. Tian, J.-Y. Xu, W. Gu, X. Liu and S.-P. Yan, *Dalton Trans*., 2010, **39**, 10637-10643; (b) G.-J. Chen, X. Qiao, C.-Y. Gao, G.-J. Xu, Z.-L. Wang, J.-L. Tian, J.-Y. Xu, W. Gu, X. Liu and S.-P. Yan, *J. Inorg. Biochem*., 2012, **109**, 90-96.
38 (a) A. Hussain and A. R. Chakravarty, *J. Chem. Sci.*, 2012, **124**, 1327-1342; (b) A. Hussain, D. Lahiri, M. S. A. Begum, S. Saha, R. Majumdar, R. R. Dighe and A. R. Chakravarty, *Inorg. Chem.*, 2010, **49**, 4036-4045; (c) A. Hussain, S. Gadadhar, T. K. Goswami, A. A. Karande and A. R. Chakravarty, *Eur. J. Med. Chem*., 2012, **50**, 319-331.
39 (a) A. Hussain, S. Gadadhar, T. K. Goswami, A. A. Karande and A. R. Chakravarty, *Dalton Trans*., 2012, **41**, 885-895; (b) A. Hussain, K. Somyajit, B. Banik, S. Banerjee, G. Nagaraju and A. R. Chakravarty, *Dalton Trans*., 2013, **42**, 182-195.
40 (a) G. Bobba, J. C. Frias and D. Parker, *Chem. Commun*., 2002, 890-891; (b) J. C. Frias, G. Bobba, M. J. Cann, C. J. Hutchison and D. Parker, *Org. Biomol. Chem*., 2003, **1**, 905-907; (c) G. Bobba, Y. Bretonnière, J.-C. Frias, *Org. Biomol. Chem*., 2003, **1**, 1870-1872; (d) R. A. Poole, G. Bobba, M. J. Cann, J.-C. Frias, D.

Parker and R. D. Peacock, *Org. Biomol. Chem*., 2005, **3**, 1013-1024.
41 K. Toshima, R. Takano, T. Ozawa and S. Matusumura, *Chem. Commun*., 2002, 212-213.
42 (a) W. D. Horrocks, Jr. and D. R. Sudnick, *J. Am. Chem. Soc.*, 1979, **101**, 334-340; (b) A. Beeby, I. M. Clarkson, R. S. Dickins, S. Faulkner, D. Parker, L. Royle, A. S. de Sousa, J. A. G. Williams and M. Woods, *J. Chem. Soc., Perkin Trans. 2*, 1999, 493-504.
43 (a) Y. Pan and C. L. Hussey, *Inorg. Chem.*, 2013, **52**, 3241-3252; (b) M. Gál, F. Kielar, R. Sokolová, Š. Ramešová and V. Kolivoška, *Eur. J. Inorg. Chem.,* 2013, 3217-3223.
44 (a) A. R. Al-Karaghouli and J. S. Wood, *Inorg. Chem.*, 1972, **11**, 2293-2299; (b) M. Fréchette, I. R. Butler, R. Hynes and C. Detellier, *Inorg. Chem.*, 1992, **31**, 1650-1656.
45 (a) A. Zalkin, D. H. Templeton and D. G. Karraker, *Inorg. Chem*., 1969, **8**, 2680-2684; (b) F. A. Saad, J. C. Knight, B. M. Kariuki and A. J. Amoroso, *Dalton Trans.*, 2013, **42**, 14826-14835.
46 (a) E. C. Long and J. K. Barton, *Acc. Chem. Res*., 1990, **23**, 271-273; (b) A. C. Komor and J. K. Barton, *Chem. Commun.*, 2013, **49**, 3617-3630.
47 (a) T. M. Kelly, A. B. Tossi, D. J. McConnell and T. C. Strekas, *Nucleic Acid Res*., 1985, **13**, 6017-6034; (b) V. A. Bloomfield, D. M. Crothers and I. Tinocoo, Jr, *Physical Chemistry of Nucleic Acids.*, Harper & Row, New York, **1974**, pp 432.
48 D. L. Boger, B. E. Fink, S. R. Brunnette, W. C. Tse and M. P. Hedrick, *J. Am. Chem. Soc.,* 2001, **123**, 5878-5891.
49 (a) M. J. Waring, *J. Mol. Biol*., 1965, **13**, 269-282; (b) B. C. Baguley and E.-M. Falkenhaug, *Nucl. Acids. Res.,* 1978, **5**, 161-171.
50 J. Ghuman, P. A. Zunszain, I. Petitpas, A. A. Bhattcharya, M. Otagiri and S. Curry, *J. Mol. Biol.*, 2005, **353**, 38-52.
51 N. S. Quiming, R. B. Vergel, M. G. Nicolas and J. A. Villanueva, *J. Health. Sci.*, 2005, **51**, 8-15.
52 (a) A. Sulkowska, *J. Mol. Struct.*, 2002, **616**, 227-232; (b) Y.-Q. Wang, H.-M. Zhang, G.-C. Zhang, W.-H. Tao and S.-H. Tang, *J. Lumin*., 2007, **126**, 211-218.
53 J. R. Lakowicz, *Principles of Fluorescence Spectroscopy*, 3rd ed., Springer: New York, 2006.
54 Y.-J. Hua, Y. Liu, J.-B. Wang, X. –H. Xiao and S.-S. Qu, *J. Pharm. Biomed. Anal.,* 2004, **36**, 915-919.
55 D. Costa, H. D. Burrows, and M. da Gracüa Miguel, *Langmuir*, 2005, **21***,* 10492-10496.
56 M. Y. Li, C. S. Cline, E. B. Koker, H. H. Carmichael, C. F. Chignell and P. Bilski, *Photochem. Photobiol*., 2001, **74**, 760-764.
57 S. M. Klein, G. Cohen and A. I. Cederbaum, *Biochemistry*, 1981, **20**, 6006-6012.
58 J. S. Beckman, T. W. Beckman, J. Chen, P. A. Marshall and B. A. Freeman, *Proc. Natl. Acad. Sci., USA,* 1990, **87**, 1620-1624.
59 (a) A. U. Khan, *J. Phys. Chem*., 1976, **80**, 2219-2228; (b) P. B. Merkel and D. R. Kearns, *J. Am. Chem. Soc.*, 1972, **94**, 1029-1030.
60 D. D. Perrin, W. L. F. Armarego and D. R. Perrin, *Purification of Laboratory Chemicals*, Pergamon Press, Oxford, 1980.
61 (a) J. E. Dickeson and L. A. Summers, *Aus. J. Chem.*, 1970, **23**, 1023-1027; (b) J. G. Collins, A. D. Sleeman, J. R. Aldrich-Wright, I. Greguric and T. W. Hambley, *Inorg. Chem.*, 1998, **37**, 3133-3141.
62 E. Amouyal, A. Homsi, J.-C. Chamron and J.-P. Sauvage, *J. Chem. Soc., Dalton Trans*., 1990, 1841-1845.
63 APEX2 v2012.4, Bruker AXS: Madison, WI, 1999.
64 N. Walker and D. Stuart, *Acta Crystallogr. A.,* 1983, **39**, 158-166.
65 G. M. Sheldrick, *SADABS, Area Detector Absorption Correction*, *University of Göttingen, Göttingen, Germany,* 2001.
66 G. M. Sheldrick, SHELX-97, *Program for Refinement of Crystal Structures*, *University of Göttingen, Göttingen, Germany*, 1997.
67 (a) G. M. Sheldrick, *Acta Crystllogr*. 2008, **A64**, 112-122; (b) G. M. Sheldrick, *SHELXTL 6.14*, Bruker, AXS Inc., Madison, WI, 2000.
68 (a) L. J. Farrugia, *WINGX ver 1.70, An Integrated System of Windows Programs for the Solution, Refinement, and Analysis of Single Crystal X-ray Diffraction Data, Department of Chemistry, University of Glasgow*, 2005; (b) L. J. Farrugia, *J. Appl. Cryst.,* 1999, **32**, 837-838.
69 M. N. Burnett and C. K. Johnson, *ORTEP-III, Report ORNL - 6895; Oak Ridge National Laboratory: Oak Ridge, TN*, 1996.
70 J. Marmur, *J. Mol. Biol.*, 1961, **3**, 208-218.
71 M. E. Reichmann, S. A. Rice, C. A. Thomas and P. Doty, *J. Am. Chem. Soc*., 1954, **76**, 3047-3053.
72 A. Wolfe, G. H. Shimer and T. Meehan, *Biochemistry*, 1987, **26**, 6392-6396.
73 M. Lee, A. L. Rhodes, M. D. Wyatt, S. Forrow and J. Hartley, *Biochemistry*, 1993, **32**, 4237-4245.
74 J. Bernadou, G. Pratviel, F. Bennis, M. Girardet and B. Meunier, *Biochemistry*, 1989, **28**, 7268-7275.

Graphical Abstract for Table of Contents

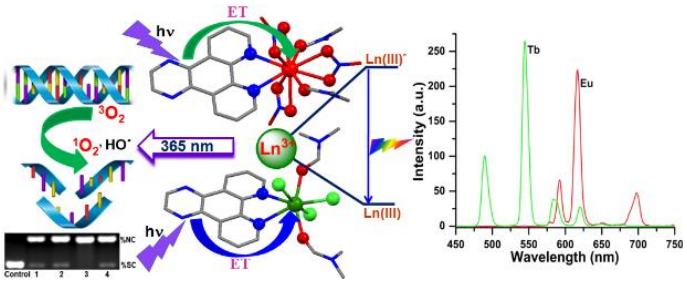

Luminescent europium and terbium complexes of quinoxaline and phenazine ligands were studied for their structures, luminescent properties, interaction with DNA, and photo-induced DNA cleavage activity.